**Supporting Information**

**Supporting Methods**

**Principal component analysis (PCA) of the covariance matrix computed from MD trajectories**

Proteins in the snapshots were iteratively superimposed onto their mean structure, <**R**>, and the covariance matrix, <$\Delta\mathbf{R}\Delta\mathbf{R}^{T}$>, is constructed using a deviation matrix **Q** and decomposed into its corresponding eigenvalues and eigenvectors such that:

$$< \Delta\mathbf{R}\Delta\mathbf{R}^{\mathrm{T}} > = (M-1)^{-1}\mathbf{Q}\mathbf{Q}^{T} = \mathbf{V}\mathbf{\Lambda}\mathbf{V}^{T} \quad \textbf{(S1)}$$

$\Delta\mathbf{R}$ is the 3$N$-dimensional deviation vector, and **Q** is the $3N \times M$ matrix, where $N$ and $M$ are, respectively, the number of protein atoms in the analysis and the number of snapshots. Each column in **Q** represents the deviation of a given snapshot from the mean structure, while each element in that column is the deviation of a given atom in the x-, y- or z-dimension. $\mathbf{V}_{3N\times 3N}$ is the eigenvector matrix containing 3$N$ eigenvectors (or principal components, PCs), each of which is 3$N$-dimensional. $\mathbf{\Lambda}$ is the $3N \times 3N$ diagonal matrix of rank-ordered eigenvalues (from large to small).

The snapshots of a trajectory are then projected onto the principal components to form a projection matrix $\mathbf{U}_{3N\times M}$ as

$$\mathbf{U} = \mathbf{V}^{\boldsymbol{T}}\mathbf{Q}$$

(**S2**)

where the row $k$ in **U,** $\mathbf{u}_k = [u_{k,0}, u_{k,1}, \ldots, u_{k,M-1}]$, contains the projections of $M$ snapshots onto a given PC eigenvector $\mathbf{V}_k$ for the $k$'th PC mode. Each snapshot of the protein structure is a scalar value (PC mode coordinate) on the mode $k$.

**Wiener–Khintchine theorem (WKT)**

In this section, we show the detailed derivations and implementations of the autocorrelation functions from the PC modes, obtained from MD simulations, using the Wiener–Khintchine theorem. For the $k^{th}$ mode and a trajectory containing $M$ snapshots, we can express the trajectory as a discrete function of time $s$ as $u_k(s) = \{u_{k0}, u_{k1}, \ldots u_{kM-1}\}$. Our goal here is to obtain the autocorrelation for the 'particle motion' (the projections of the MD snapshots) at the $n^{th}$ time point. In statistical mechanics, it is, by definition, the ensemble average of the correlation of particle positions at a time shift $t \equiv n\Delta t$, where $\Delta t$ is the time step. For long-enough equilibrium simulation, the ensemble average can be replaced by the time average under the ergodic hypothesis such that

$$C_k(t) \equiv < u_k(s)u_k(t+s) >$$
$$= < u_k(s)u_k(n\Delta t + s) >$$

$$\approx \frac{1}{M-n}\sum_{i=1}^{M-n} u_k(s_i)u_k(s_i+n\Delta t)$$

(**S3**)

where $s_i$ is the time point when we start to calculate the time-correlation between the $u_k$ at $s_i$ and the $u_k$ after $n$ time-steps; $n$ goes from 0 to ($M$ – 1). The summation runs from 1 to ($M$ – $n$) time point since we are only interested in a $n$-time-step shift. The computation time of such a calculation grows with $O(M^2)$ for all the possible $t$ to be obtained. Long computation time is inevitable especially for a long trajectory, repeated for many modes ($3N$ – 6, where $N$ is the degrees of freedom being analyzed). For our purpose here as well lessening the computational burden, we want to obtain the time-correlation function by first Fourier transforming snapshot projections on a given mode into their counterparts in the frequency domain, and then inverse transform the power spectrum back to obtain the $C_k(t)$. This mathematical treatment is known as Wiener–Khintchine theorem[1] in statistical mechanics, which proves that the autocorrelation function is equal to the inverse Fourier transformation of the power spectrum of the trajectories such that

$$C_k(t) = \frac{1}{2M}\sum_{f=0}^{2M-1} S_k(f)\, e^{\frac{2\pi i f t}{2M}}$$

(**S4**)

where power spectrum $S_k(\omega)$ is defined as the magnitude of the Fourier transformation of snapshot projections on the $k^{th}$ PC mode $\widetilde{u_k}(\omega) = \{\widetilde{u_{k0}}, \widetilde{u_{k1}}, \ldots \widetilde{u_{k2M-1}}\}$, such that $S_k(\omega) = \{|\widetilde{u_{k0}}|^2, |\widetilde{u_{k1}}|^2, \ldots |\widetilde{u_{k2M-1}}|^2\}$. There are $2M$ components in $u_k(s)$ instead of $M$ components after

we pad $M$ zeros after the original $M$ $u_k$ projections such that $u_k(s) = \{u_{k0}, u_{k1}, \ldots u_{kM-1}, 0^1, 0^2, \ldots 0^M\}$. This is to make sure that we obtain $M$ positive frequency values.

In addition, one can notice that in the last line of **eq S3**, termed as brute force method herein, for the $n^{th}$ value of correlation function, the summation goes from 1 to ($M - n$), leading to less addends in the summation as $n$ increases. Therefore, we need to pad enough zeros at the end of the time series as the input of DFT in order to make sure the Fourier transformation reproduces correct results. In our case, we pad $M$ zeros in the end of the sequence so that after the inverse transformation we get back a sequence of length $2M$. For our needs, we only take the sequence in the positive time domain, with $M$ time points. The comparison between Wiener–Khintchine theorem and the brute force method shows that Wiener–Khintchine theorem can indeed reproduce correct time correlation functions, evident that our method is applicable in computing autocorrelation functions with a time complexity of $O(M \ln M)$.

**Intensity-Weighted Period (IWP), Relaxation Time and Characteristic Time**

The IWP for a specific PC mode $k$ is computed as

$$\tau_{w,k} = \frac{2\pi \sum_{i=1}^{M} S_k(\omega_i)\omega_i{}^{-1}}{\sum_{j=1}^{M} S_k(\omega_j)} \quad \textbf{(S5)}$$

where $S_k(\omega_i)$ is the power for the angular frequency, $\omega_i$.

While, the relaxation of $C_k(t)$ is modeled as an exponential function

$$C_k(t) = A \exp\left(-\frac{t}{\tau_r}\right) \quad \textbf{(S6)}$$

The values of $C_k(t)$ from unity (when $t = 0$) to the first instance that the function reaches zero ($<10^{-5}$) were used to fit the exponential and obtain $\tau_r$.

The characteristic time is defined as

$$\tau_c = \frac{\sum_{i=1}^{M} C_k(t_i)\Delta t}{C_k(0)} \quad \textbf{(S7)}$$

where $\Delta t = 0.1$ ps is the time interval between two consecutive snapshots.

**Fluctuation Profile Matching (FPM)**

FPM takes 2 profiles of the same dynamics variable and assesses their degree of agreement via Pearson's correlation coefficient[2], which ranges from -1 to 1.

**Theoretical Covariance Matrix from MD with Removed PC Modes**

The eigenvectors and eigenvalues are obtained as per **eq S1** with the first *k*-1 modes (lower PC modes have larger variances or eigenvalues) removed such that

$$< \Delta\mathbf{R}\Delta\mathbf{R}^{\boldsymbol{T}} >_{MD,k} = \sum_{a=k}^{3N-6} \lambda_a \mathbf{V}_a \mathbf{V}_a{}^{\boldsymbol{T}} \quad \textbf{(S8)}$$

where $\mathbf{V}_a$ is the eigenvector with its corresponding eigenvalue, $\lambda_a$, taken from the diagonal of $\mathbf{\Lambda}$ in **eq S1** for the *a*'th PC mode.

**RMSF and ADP Profiles for Ubiquitin from X-ray Structure, NMR Structures and MD**

The $RMSF_{exp}$ profile was calculated by treating the ensemble of 32 NMR-determined conformers (PDB ID: 1G6J) of ubiquitin (Cα atoms only) as snapshots and obtaining the $<\Delta\mathbf{R}\Delta\mathbf{R}^{\boldsymbol{T}}>_{exp,1G6J}$ matrix by **eq S1**. Then the RMSF of each residue is the square-root of the sum of the x-, y- and z-dimension variances for the respective residues taken from the diagonal of $<\Delta\mathbf{R}\Delta\mathbf{R}^{\boldsymbol{T}}>_{exp,1G6J}$. The $RMSF_{MD,k}$ profile is computed using the same method but with their respective $<\Delta\mathbf{R}\Delta\mathbf{R}^{\boldsymbol{T}}>_{MD,k}$ matrix in **eq S8**.

To obtain $ADP_{exp}$, the Cα atoms of the ubiquitin X-ray structure PDB ID: 2GBJ (chain B) is superimposed onto the mean structure of MD snapshots. The rotation matrix $\mathbf{R'}_{3\times3}$ used to remove rotational differences between the 2 structures is obtained. Then, the ADP matrix, $\mathbf{U'}_{3\times3}$, for each residue is rotated to obtain the superimposed ADP matrices $(\mathbf{R'U'R'}^{\boldsymbol{T}})^3$. From the ADP matrix,

the ADP dynamical variable of each residue consisting of 3 variance components and 3 unique covariance components (the xy- and yx- components are the same and so are xz- and zx-components, etc.) are extracted to form the 6*N*-dimensional $ADP_{exp}$ profile.

While, the ADP matrix from MD for each Cα atom is the atom's x-, y- and z-dimension covariance matrix extracted from the full $<\Delta\mathbf{R}\Delta\mathbf{R}^{\mathbf{T}}>_{MD,k}$ matrix. The component of this matrix was extracted exactly as above to form the $ADP_{MD,k}$ profile.

**Order Parameter Profiles derived from NMR-determined structural ensemble and MD snapshots**

$S^2$ describes the order of the backbone -NH bond vector $r_{ij} = (x_{ij}, y_{ij}, z_{ij})$ pointing from atom *i* to *j* (herein, *i* is N, and *j* is H) which can be approximated as[4–6]

$$S_{ij}^2 = \frac{3}{2}\left(< x_{ij}^2 >^2 + < y_{ij}^2 >^2 + < z_{ij}^2 >^2 + 2 < x_{ij}y_{ij} >^2 + 2 < x_{ij}z_{ij} >^2 + 2 < y_{ij}z_{ij} >^2\right) - \frac{1}{2} \quad \textbf{(S9)}$$

Here, the length of $r_{ij}$ is normalized to unity. The angular brackets denote averages taken over the *M* snapshots; herein *M* = 6,000,000 or 1,200,000 are for the 600 ns and 120 ns trajectories, respectively.

To obtain the MD-derived $S^2_{MD,k}$ profile for all the PC modes ≥ $k^{th}$ mode, the protein structure in each snapshot is rebuilt using all the PC modes ≥ $k^{th}$ mode which is then used to obtain the -NH bond vectors for calculating $S^2_{MD,k,ij}$ with **eq S9**.

The method used to rebuild the structures as a function of constituent modes is as follows, for ubiquitin's structure in snapshot *m*, the coordinates of its atoms ($\mathbf{R}_m$) can be expressed as

$$\mathbf{R}_m = <\mathbf{R}> + \sum_{a=1}^{3N-6} \left((\mathbf{R}_m - <\mathbf{R}>) \cdot \mathbf{V}_a\right)\mathbf{V}_a \quad \textbf{(S10)}$$

Then, the atom coordinates of snapshot *m* rebuilt using all the PC modes ≥ $k^{th}$ mode can be obtained by the following equation

$$\mathbf{R}_{m,k} = <\mathbf{R}> + \sum_{a=k}^{3N-6} \left((\mathbf{R}_m - <\mathbf{R}>) \cdot \mathbf{V}_a\right)\mathbf{V}_a \quad \textbf{(S11)}$$

where <**R**> represents the mean coordinate of the structure over *M* snapshots, and $\mathbf{V}_a$ is the $a^{th}$ PC eigenvector.

Now, for each snapshot $\mathbf{R}_{m,k}$, we compute the normalized NH bond vector $r_{ij}$ for every residue (except for prolines). The averages of $x_{ij}^2$, $y_{ij}^2$, $z_{ij}^2$, $x_{ij}y_{ij}$, $x_{ij}z_{ij}$ and $y_{ij}z_{ij}$ over the whole trajectory were calculated and used to obtain $S^2_{MD,k,ij}$.

The experimental order parameters, $S^2_{exp}$, for ubiquitin were taken from Tjandra et al[7].

**Derivation of General Elastic Network Model (ENM) – the relation between covariance and Hessian**

In the equilibrium state, the protein system is harmonically approximated and assumed to have the Hamiltonian

$$H_0 = \frac{1}{2}\mathbf{p}^T\mathbf{M}^{-1}\mathbf{p} + \frac{1}{2}\Delta\mathbf{R}^T\mathbf{H}\Delta\mathbf{R} \quad \textbf{(S12)}$$

Where $\mathbf{p}$ is the $3N\times1$ momentum vector in the Cartesian coordinate system, and $\mathbf{M}^{-1}$ is the inverse of a $3N\times3N$ diagonal mass matrix comprising elements of triplicate mass of every node[8–10]. The superscript $T$ denotes matrix transposition. $\Delta\mathbf{R}$ is a $3N\times1$ displacement vector and $\mathbf{H}$ is the symmetric Hessian matrix, or, the force constant tensor of the system, and have the meaning of coupling force constants in each pairwise connected degrees of freedom.

Here we note that since $\mathbf{H}$ is diagonalizable, for the ease of the following derivations of the ensemble average of positional covariance, we transform $\mathbf{H}$ in normal-mode space, such that

$$\begin{aligned}\Delta\mathbf{R}^T\mathbf{H}\Delta\mathbf{R} &= \Delta\mathbf{R}^T(\mathbf{U}\mathbf{D}\mathbf{U}^T)\Delta\mathbf{R} \\ &= (\mathbf{U}^T\Delta\mathbf{R})^T\mathbf{D}(\mathbf{U}^T\Delta\mathbf{R}) \\ &= \mathbf{q}^T\mathbf{D}\mathbf{q}\end{aligned}$$

(**S13**)

Where **D** is the diagonal eigenvalue matrix, **U** is the unitary eigenvector matrix and **q** is the displacement vector in normal-mode space with the relationship $\mathbf{q} = \mathbf{U}^T\Delta\mathbf{R}$.

Since unitary transformation conserves length so that we can change the integration to normal-mode space, which is readily solvable.

Now, from **eqs S12 and S13**, we write $H_0$ in the expanded form as

$$H_0 = \frac{1}{2}\mathbf{p}^T\mathbf{M}^{-1}\mathbf{p} + \frac{1}{2}\mathbf{q}^T\mathbf{D}\mathbf{q} = \frac{1}{2}\sum_{k=1}^{3N}\frac{p_k^2}{m_k} + \frac{1}{2}\sum_{k'=1}^{3N}\lambda_{k'}q_{k'}^2$$

(**S14**)

In the above expression, *k* and *k'* represent the index through all 3*N* degrees of freedom, and $m_k$ is the mass elements in **M** with *N* triplicates.

In canonical ensemble we write down the partition function with phase space formulation and solve it by expanding all the terms

$$Z_0 = \iint e^{-\beta\left(\frac{1}{2}\mathbf{p}^T\mathbf{M}^{-1}\mathbf{p} + \frac{1}{2}\mathbf{q}^T\mathbf{D}\mathbf{q}\right)}\, d^{3N}\mathbf{p}\, d^{3N}\mathbf{q}$$

$$= \int e^{-\frac{\beta}{2}\mathbf{p}^T\mathbf{M}^{-1}\mathbf{p}}\, d^{3N}\mathbf{p} \int e^{-\frac{\beta}{2}\mathbf{q}^T\mathbf{D}\mathbf{q}}\, d^{3N}\mathbf{q}$$

$$= \int_{-\infty}^{\infty} \dots \int_{-\infty}^{\infty} e^{-\frac{\beta}{2}\sum_{k=1}^{3N}\frac{p_k^2}{m_k}}\, dp_1 dp_2 \dots dp_{3N} \int_{-\infty}^{\infty} \dots \int_{-\infty}^{\infty} e^{-\frac{\beta}{2}\sum_{k'=1}^{3N}\lambda_{k'}q_{k'}^2}\, dq_1 dq_2 \dots dq_{3N}$$

$$= \prod_{n=1}^{N}\left[\left(\int_{-\infty}^{\infty} e^{-\frac{\beta p_n^2}{2m_n}}\, dp_n\right)^3\right] \prod_{k'=1}^{3N}\left[\int_{-\infty}^{\infty} e^{-\frac{\beta\lambda_{k'}q_{k'}^2}{2}}\, dq_{k'}\right]$$

$$= \prod_{n=1}^{N}\left[\left(\frac{2\pi m_n}{\beta}\right)^{\frac{3}{2}}\right] \sqrt{\frac{(2\pi)^{3N}}{\beta^{3N}(\lambda_1\lambda_2 \dots \lambda_{3N})}}$$

$$= \left(\frac{2\pi}{\beta}\right)^{\frac{3N}{2}} (m_1 m_2 \dots m_N)^{\frac{3}{2}} \sqrt{\frac{(2\pi)^{3N}}{\beta^{3N}\det\mathbf{H}}}$$

(**S15**)

where $\beta=1/k_BT$; $k_B$ is the Boltzmann constant and $T$ is the absolute temperature.

In the equation above we use the property that for a symmetric matrix the product of its eigenvalues is the determinant of itself.

To calculate the positional covariance, we note one derivative

$$\frac{\partial(\Delta\mathbf{R}^T\mathbf{H}\Delta\mathbf{R})}{\partial H_{ij}} = \frac{\partial[\sum_{k=1}^{3N}\Delta R_k(\sum_{l=1}^{3N}H_{kl}\Delta R_l)]}{\partial H_{ij}}$$

$$= \Delta R_i \frac{\partial(\sum_{l=1}^{3N}H_{il}\Delta R_l)}{\partial H_{ij}}$$

$$= \Delta R_i \frac{\partial H_{ij}}{\partial H_{ij}}\Delta R_j$$

$$= \Delta R_i \Delta R_j$$

$$= (\Delta\mathbf{R}\Delta\mathbf{R}^T)_{ij}$$

**(S16)**

Now

$$\langle\Delta\mathbf{R}\Delta\mathbf{R}^T\rangle = \frac{\iint \Delta\mathbf{R}\Delta\mathbf{R}^T e^{-\beta\left(\frac{1}{2}\mathbf{p}^T\mathbf{M}^{-1}\mathbf{p}+\frac{1}{2}\Delta\mathbf{R}^T\mathbf{H}\Delta\mathbf{R}\right)} d^{3N}\mathbf{p}\, d^{3N}\Delta\mathbf{R}}{Z_0}$$

$$= \frac{\iint \Delta\mathbf{R}\Delta\mathbf{R}^T e^{-\beta\left(\frac{1}{2}\mathbf{p}^T\mathbf{M}^{-1}\mathbf{p}+\frac{1}{2}\Delta\mathbf{R}^T\mathbf{H}\Delta\mathbf{R}\right)} d^{3N}\mathbf{p}\, d^{3N}\Delta\mathbf{R}}{\iint e^{-\beta\left(\frac{1}{2}\mathbf{p}^T\mathbf{M}^{-1}\mathbf{p}+\frac{1}{2}\Delta\mathbf{R}^T\mathbf{H}\Delta\mathbf{R}\right)} d^{3N}\mathbf{p}\, d^{3N}\Delta\mathbf{R}}$$

**(S17)**

For each element in the covariance matrix

$$\langle\Delta\mathbf{R}\Delta\mathbf{R}^T\rangle_{ij} = \frac{\iint (\Delta\mathbf{R}\Delta\mathbf{R}^T)_{ij} e^{-\beta\left(\frac{1}{2}\mathbf{p}^T\mathbf{M}^{-1}\mathbf{p}+\frac{1}{2}\Delta\mathbf{R}^T\mathbf{H}\Delta\mathbf{R}\right)} d^{3N}\mathbf{p}\, d^{3N}\Delta\mathbf{R}}{\iint e^{-\beta\left(\frac{1}{2}\mathbf{p}^T\mathbf{M}^{-1}\mathbf{p}+\frac{1}{2}\Delta\mathbf{R}^T\mathbf{H}\Delta\mathbf{R}\right)} d^{3N}\mathbf{p}\, d^{3N}\Delta\mathbf{R}}$$

$$= -\frac{2}{\beta}\frac{\partial}{\partial H_{ij}}\ln Z_0$$

$$= -\frac{2}{\beta}\frac{\partial}{\partial H_{ij}}\left(\frac{3N}{2}\ln\frac{2\pi}{\beta} + \frac{3}{2}\ln(m_1 m_2 \dots m_N)\right.$$

$$\left. + \frac{3N}{2}\ln\frac{2\pi}{\beta} - \frac{1}{2}\ln\det\mathbf{H}\right)$$

$$= \frac{1}{\beta}\frac{1}{\det\mathbf{H}}\frac{\partial\det\mathbf{H}}{\partial H_{ij}}$$

$$= \frac{1}{\beta}\frac{1}{\det\mathbf{H}}\frac{\partial\left(\sum_{k=1}^{3N} H_{ik}C_{ik}\right)}{\partial H_{ij}}$$

$$= \frac{1}{\beta}\frac{1}{\det\mathbf{H}}\sum_{k=1}^{3N}\delta_{jk}C_{ik}$$

$$= \frac{1}{\beta}\frac{1}{\det\mathbf{H}}C_{ij}$$

$$= \frac{1}{\beta}\frac{1}{\det\mathbf{H}}[(\mathrm{adj}\mathbf{H})^T]_{ij}$$

$$= \frac{1}{\beta}\frac{1}{\det\mathbf{H}}\left[\det\mathbf{H}\cdot(\mathbf{H}^{-1})_{ij}^T\right]$$

$$= \frac{1}{\beta}(\mathbf{H}^{-1})_{ij}$$

(**S18**)

Where $C_{ik}$ in the above derivation is the *ik*-element of the cofactor matrix of the Hessian. Here we use Laplace formula to expand the Hessian determinant and using the properties that (1) the adjugate matrix is the transpose of cofactor matrix, (2) inverse of any nonsingular matrix **A** is $\mathbf{A}^{-1} = \frac{1}{\det\mathbf{A}}\mathrm{adj}\mathbf{A}$ and (3) the inverse of any symmetric matrix, in our case Hessian, is still symmetric.

Finally, in matrix form we write

$$\langle\Delta\mathbf{R}\Delta\mathbf{R}^T\rangle = \frac{1}{\beta}\mathbf{H}^{-1}$$

(**S19**)

which is the expected result by analogy to one-dimensional harmonic oscillator system.

This result holds true for all types of ENMs as long as the system is harmonically approximated. For ENMs that have translational and/or rotational invariance[10], which makes the rank of **H** less than its dimension, $\mathbf{H}^{-1}$ is solved by eigenvalue decomposition followed by removing the terms containing zero eigenvalues.

**The Anisotropic Network Model (ANM)**

The Anisotropic Network Model (ANM) is a type of ENM with the following potential energy function

$$U_{ANM} = \sum_{i.j=1}^{N} \frac{\gamma}{2}\left(L_{ij} - L_{ij}^{0}\right)^{2}\theta\left(r_c - L_{ij}^{0}\right) = \frac{1}{2}\Delta\mathbf{R}^{T}\mathbf{H}\Delta\mathbf{R} \qquad (\mathbf{S20})$$

where the index $i$ and $j$ represents the nodes (Cα atoms) that runs from 1 to $N$. The γ represents the universal spring constant of the system. $L_{ij}$ is the current distance between the $i^{th}$ and $j^{th}$ nodes while $L_{ij}^{0}$ is the equilibrium distance between $i$ and $j$. When $L_{ij}^{0}$ is $\leq r_c$, the cut-off distance, then these two nodes are treated as connected. This is expressed as a Heaviside-step function $\theta$ in **eq S20**.

All the elements of the Hessian matrix **H** can be calculated as the second derivative of the potential energy function. Details of this can be found in the supplementary information of our previous

work[10]. The eigenvector ($\boldsymbol{V}_{ANM}$) and eigenvalue ($\lambda_{ANM}$) of each ANM mode is calculated from the eigen-decomposition of **H such that**

$$< \Delta\mathbf{R}\Delta\mathbf{R}^{\boldsymbol{T}} >_{ANM} = \frac{k_B T}{\gamma} \sum_{a=6}^{3N} \lambda_a^{-1} \mathbf{V}_a \mathbf{V}_a^{\boldsymbol{T}} \quad \textbf{(S21)}$$

ANM analysis can be performed on the DynOmics Portal 1.0[11]:

http://dyn.life.nthu.edu.tw/oENM/.

**Theoretical Covariance Matrix, RMSF and ADP from ANM With Removed Modes**

The ANM derived covariance matrix for all ANM modes ≥ $l$ (lower ANM modes have lower frequencies or smaller eigenvalues) can be calculated as follows

$$< \Delta\mathbf{R}\Delta\mathbf{R}^{\boldsymbol{T}} >_{ANM,l} = \frac{k_B T}{\gamma} \sum_{a=l+6}^{3N} \lambda_a^{-1} \mathbf{V}_a \mathbf{V}_a^{\boldsymbol{T}} \quad \textbf{(S22)}$$

where $\boldsymbol{V}_a$ and $\lambda_a$ are the eigenvector and eigenvalue of the $a$'th ANM mode.

The $RMSF_{ANM,l}$ and $ADP_{ANM,l}$ profiles were computed from the $<\Delta\mathbf{R}\Delta\mathbf{R}^{\boldsymbol{T}}>_{ANM,l}$ matrix with the same methods used for MD-derived profiles of RMSF and ADP.

**ANM Mode Time Scale Assignment Through ANM-PCA Mode Mapping**

Every ANM mode $l$ was mapped to a PC mode $k^*$ from MD by comparing the $RMSF_{ANM,l}$ with the $RMSF_{MD,k}$ profiles for different $k$'s using FPM to identify the $k = k^*$ with the highest correlation. Every ANM mode $l$ was then assigned the IWP ($\tau_{w,k^*}$) of the mapped PC mode $k^*$.

The ANM-PCA mode mapping might result in a PC mode getting mapped to multiple ANM modes. The ANM mode with the highest correlation with the PC mode was kept while the rest were removed. This filtered set of ANM-PCA mode mapping was used to fit the power laws.

**Fitting the Time Power Laws**

The relationship between an ANM mode's eigenvalue ($\lambda_{ANM}$) and mapped time scale ($t_{ANM}$) was modeled as a power law in the form of $t_{ANM} = c \times \lambda_{ANM}^{d}$, with the constants $c$ and $d$ to be found through the fitting procedure described below.

The natural log of the power law, $\ln(t_{ANM}) = \ln(c) + d \ln(\lambda_{ANM})$, was used to get a linear function of $\ln(t_{ANM})$ with respect to $\ln(\lambda_{ANM})$. Least squares fitting was then used to obtain the parameters $c$ and $d$.

**Fitting the Variance Power Law**

Given the mapping between ANM modes and PCA modes, the $\lambda_{ANM}$ and $\lambda_{PCA}$ (PC mode's eigenvalue/variance) were used to fit a variance power law such that $\lambda_{PCA} = a \times \lambda_{ANM}^{b}$, where $a$ and $b$ are constants. The constants were found by following the same procedure used to fit the time power laws.

**Identifying the Functional Modes Corresponding to Ribosomal Body Rotation (Ratcheting) and Head Swiveling Motions**

The ribosomal ratcheting motion is the relative body rotation between the 30S and 50S subunits of the ribosome. The axis of rotation, $\mathbf{r}_B$, is assumed to be the vector connecting the COMs of the 2 subunits as observed in the non-rotated x-ray crystallographically resolved conformation (PDB ID: 4V6F). While for the head swiveling motion's axis of rotation, $\mathbf{r}_H$, it is the vector between the COMs of the 30S body and 30S head. Where the 30S head is defined as the residues 921-1396 of the 16S rRNA complexed with the ribosomal proteins S3, S7, S9, S10, S13, S14, S19 and Thx. While, the 30S body is defined as residues 5-920 and 1399-1543 of the 16S rRNA complexed with ribosomal proteins S2, S4, S5, S6, S8, S11, S12, S15, S16, S17, S18 and S20.

ANM analysis was performed on the non-rotated x-ray solved conformation. The $k^{\text{th}}$ ANM eigenvector ($\mathbf{V}_k$) was used to deform the non-rotated conformation by

$$\mathbf{R}_k = \mathbf{R}_0 \pm \sqrt{k_B T/\gamma}\mathbf{V}_k \quad \textbf{(S23)}$$

where $\mathbf{R}_0$ is a $3N$ vector containing the coordinates of the $N$ atoms in the non-rotated conformation and $\mathbf{R}_k$ is the conformation deformed from $\mathbf{R}_0$ along the $k^{\text{th}}$ ANM mode by setting $k_BT/\gamma$ to be unity. For the purpose of obtaining axis of rotation, the results do not change as long as $k_BT/\gamma$ is set to be a small value.

The ratcheting motion is relative to the 50s subunit and therefore the deformed conformation was first superimposed at the 50S subunit. To capture the head swiveling motion, we superimposed the deformed conformation at the 50S subunit and 30S' body part to avoid capturing the ratcheting motion and examined the rotation of 30S head.

Considering the transition from non-rotated ($\mathbf{R_0}$) to deformed conformation ($\mathbf{R_k}$) takes place at a time interval $\Delta t$ (in seconds), the angular momentum vector ($\mathbf{L}_k$) for the $k^{\text{th}}$ mode is the cross product between the mass-weighted position of atoms and atom velocity, such that

$$\mathbf{L}_k = \sum_i m_i \mathbf{R}_{0,i} \times \mathbf{v}_{k,i} \qquad \textbf{(S24)}$$

where $\mathbf{R}_{0,i}$ is the $i^{\text{th}}$ atom's position vector in the non-rotated conformation, $m_i$ is the atom mass of $i$ and the velocity vector $\mathbf{v}_{k,i} = (\mathbf{R}_{k,i} - \mathbf{R}_{0,i})/\Delta t$ where $\mathbf{R}_{k,i}$ is the position vector of atom $i$ in the conformation deformed along the $k^{\text{th}}$ mode.

$\mathbf{L}_k$ is related to the angular velocity vector ($\boldsymbol{\omega}_k$) by

$$\mathbf{L}_k = \mathbf{I}\boldsymbol{\omega}_k$$

$$\boldsymbol{\omega}_k = \mathbf{I}^{-1}\mathbf{L}_k$$

$$\boldsymbol{\omega}_k \Delta t = \mathbf{I}^{-1}\mathbf{L}_k \Delta t = \mathbf{I}^{-1} \sum_i m_i \mathbf{R}_{0,i} \times \left(\mathbf{R}_{k,i} - \mathbf{R}_{0,i}\right)$$

(**S25**)

The direction of $\boldsymbol{\omega}_k$ is the *axis of rotation* for mode *k* while $|\boldsymbol{\omega}_k|$ is the angular velocity in the unit of radians/second and therefore $|\boldsymbol{\omega}_k|\Delta t$ gives us the angle of rotation in radians (the length of $\Delta t$ does not change the result).

The deviation angle $\theta$ between $\mathbf{r}_{B\ or\ H}$ and rotation axis $\boldsymbol{\omega}_k$ from mode *k* were computed for the slowest 50 ANM modes, where $\cos\theta = (\mathbf{r}_{B\ or\ H} \cdot \boldsymbol{\omega}_k)/(\|\mathbf{r}_{B\ or\ H}\|\|\boldsymbol{\omega}_k\|)$. The mode with the smallest angle deviating from $\mathbf{r}_B$ (or $\mathbf{r}_H$) was chosen as the functional mode ($k^f$) for the ratcheting (or for swiveling) motion.

**Predicting the Conformation of the Ribosome After the Ratcheting and Head Swiveling Motions**

After identifying the ANM mode ($k^f$) that corresponds to the body rotation/head swiveling motion, the conformation of the ribosome could be obtained by

$$\mathbf{R}_{k^f} = \mathbf{R}_0 \pm \sqrt{{\sigma_{k^f}}^2}\mathbf{V}_{k^f}$$

(**S26**)

where variance ( $\sigma_{k^f}^2$ ) of mode $k^f$ can be predicted by the variance power law $\sigma_{k^f}^2 = 46.0538\ \lambda_{k^f}^{-2.5085}$ with $\lambda_{k^f}$, the eigenvalue of mode $k^f$.

**Identifying the Functional Modes and Conformations Corresponding to the L1 Stalk Closing Motion**

To identify the L1 stalk's functional mode and conformation, the non-rotated ribosome (PDB ID: 4V6F) was first deformed along all 50 modes using the variance power law as in **eq S26**. The deformed conformations were then superimposed at the 50S subunit as described above. Finally, we identify the mode with the shortest distance between the COM of the deformed L1 stalk and the E-site in the non-rotated ribosome. The L1 stalk is defined as the helices 76-78 (residues 2093-2196) of the 23S rRNA complexed with L1 protein and the COM of E-site is defined by the COM of E-site tRNA as observed in the non-rotated ribosome (PDB ID: 4V6F).

## Supporting Figures

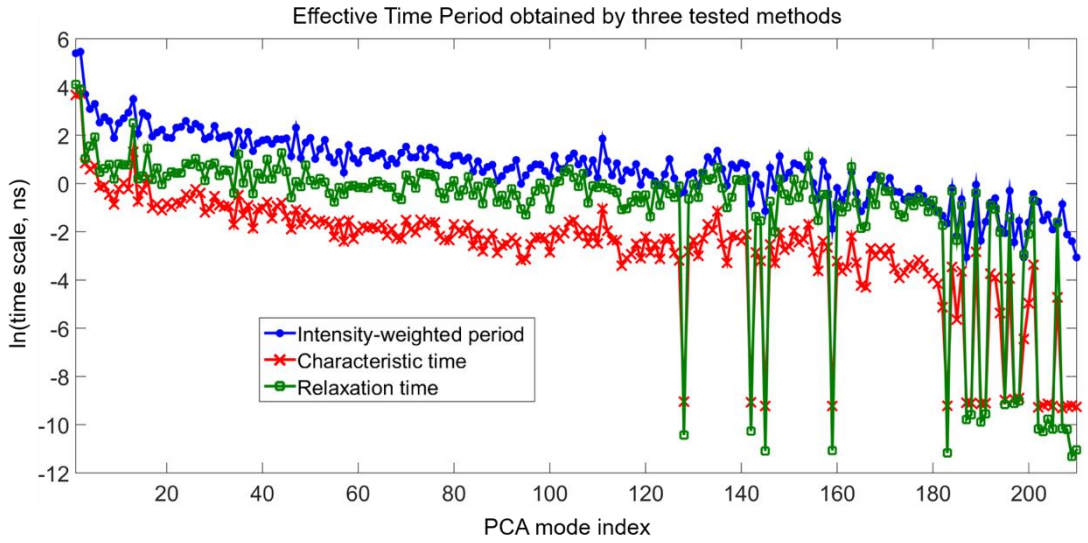


**Figure S1. Time scale of each PC mode of ubiquitin estimated using the three tested methods.** There are $3 \times 72 - 6 = 210$ PC modes ($C_\alpha$-based) calculated from the 600-nanosecond simulation of ubiquitin. The blue, red and green lines show intensity-weighted period ($\tau_w$), characteristic time ($\tau_c$) and relaxation time ($\tau_r$) respectively for all the PC modes.

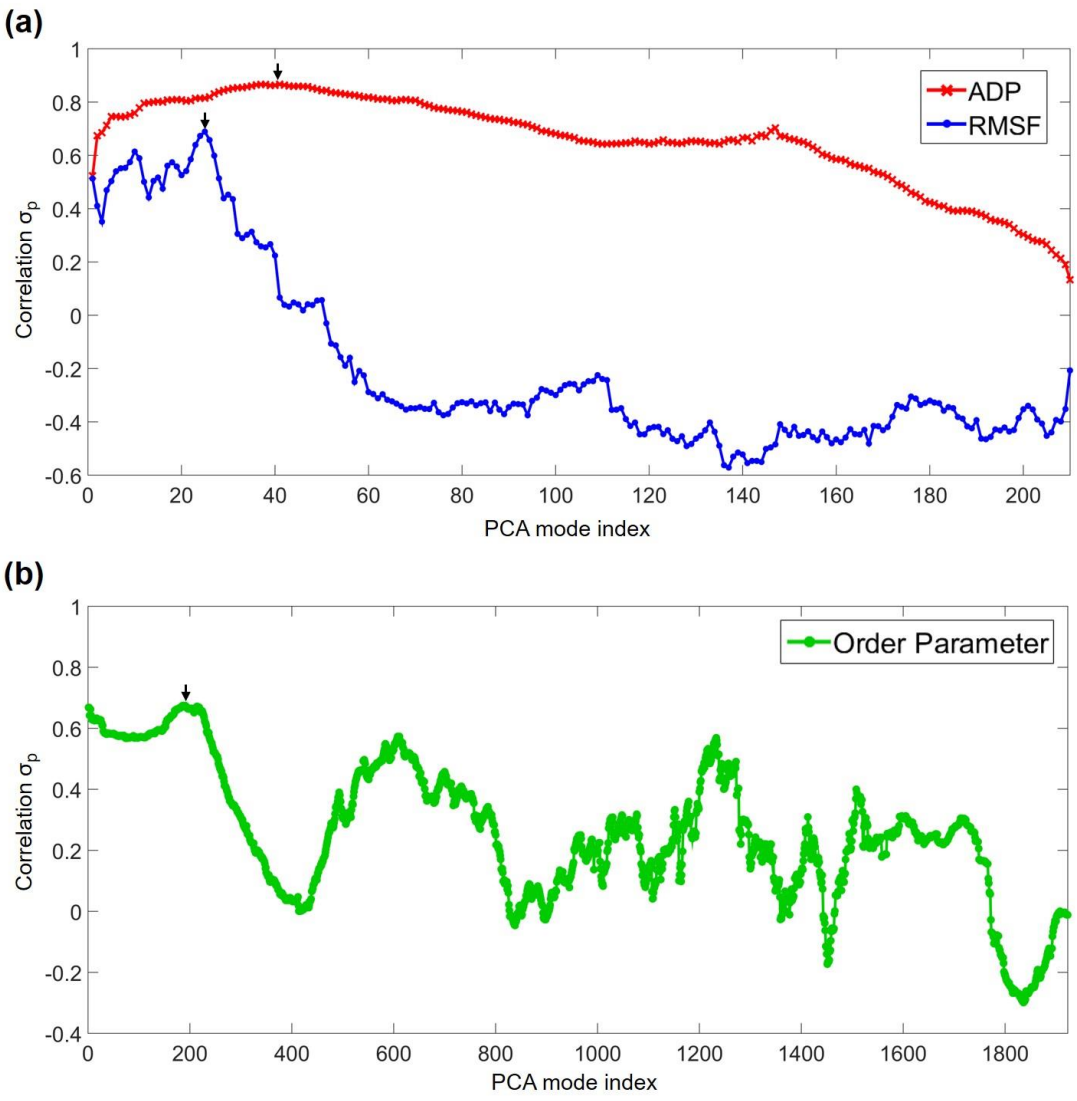


**Figure S2. The PC modes that best match the dynamics variables of ubiquitin. (a)** The Pearson correlation coefficient between the anisotropic displacement parameters (ADP) profile assembled from all the PC modes higher or equal to a specific mode with the experimental ADP profile (PDB: 2GBJ) is shown in red crosses. Blue circles give correlation coefficients between RMSF profile derived from covariance comprising PC modes higher or equal to a given mode (**eq S8**) and RMSF derived from a set of NMR-determined conformers (PDB: 1G6J). In **(a)**, the PC modes are calculated using only Cα atoms (coarse-grained). **(b)** Pearson correlation coefficient between experimental NMR order parameters and order parameters estimated from the PCA of heavy-

atoms with the backbone nitrogen's hydrogen atom. The black arrow indicates the PC mode with the highest correlation.

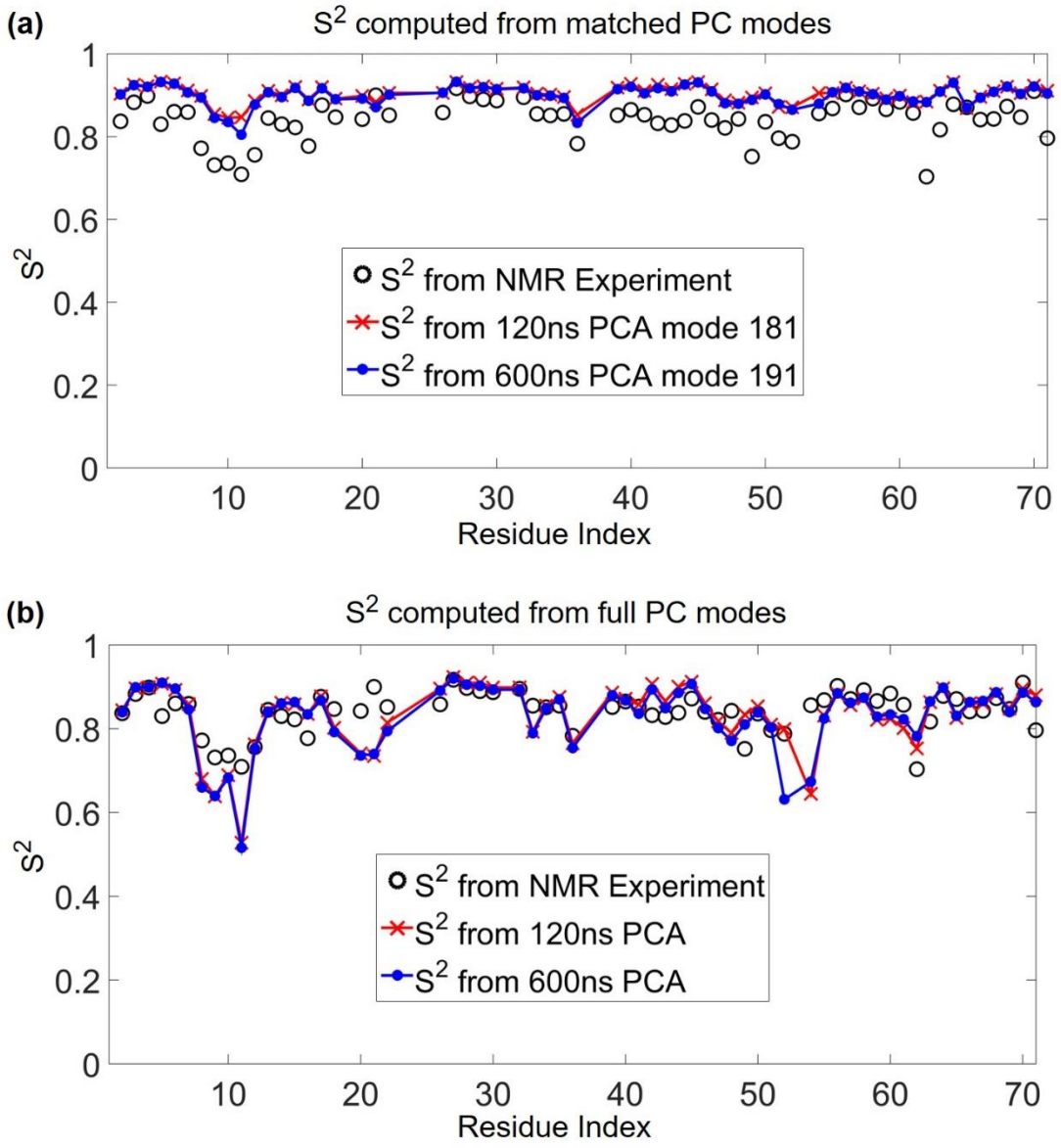


**Figure S3. NMR Order parameters ($S^2$) estimated from the 120 ns and 600 ns MD trajectories. (a)** The profiles are the order parameters derived from PC modes ($k$=181 and 191 for 120 and 600ns simulations, respectively) that best-match the experimental data. One can obtain the time scales of 1.0 ns and 2.3 ns for the NMR-characterized $S^2$ profile from the best-matched mode 181 and 191, respectively. **(b)** The profiles are order parameters derived from full PC modes ($k$=1 in **eq S9**). It is readily understandable that the longer the simulation is, the wider the spatial distribution (and therefore less order) of an atom would result.

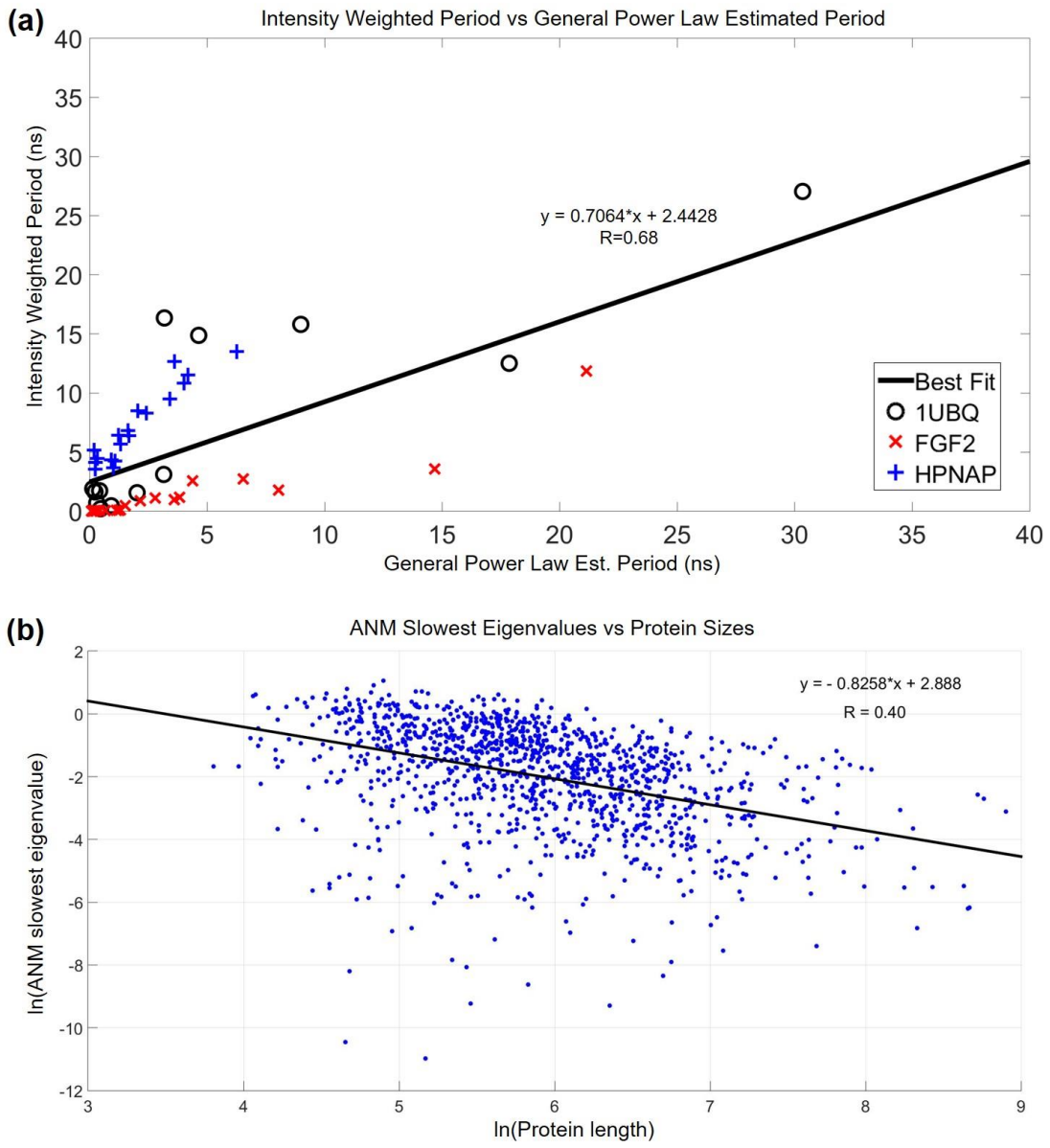


**Figure S4. (a)** The IWPs are compared to the power-law estimated periods for the combined ANM modes of ubiquitin, FGF2 and HPNAP ($\sigma_p = 0.68$). **(b)** The ANM eigenvalues of the slowest modes are plotted against protein sizes (the number of residues in a protein) for a previously published set of non-homologous 1228 proteins[12].

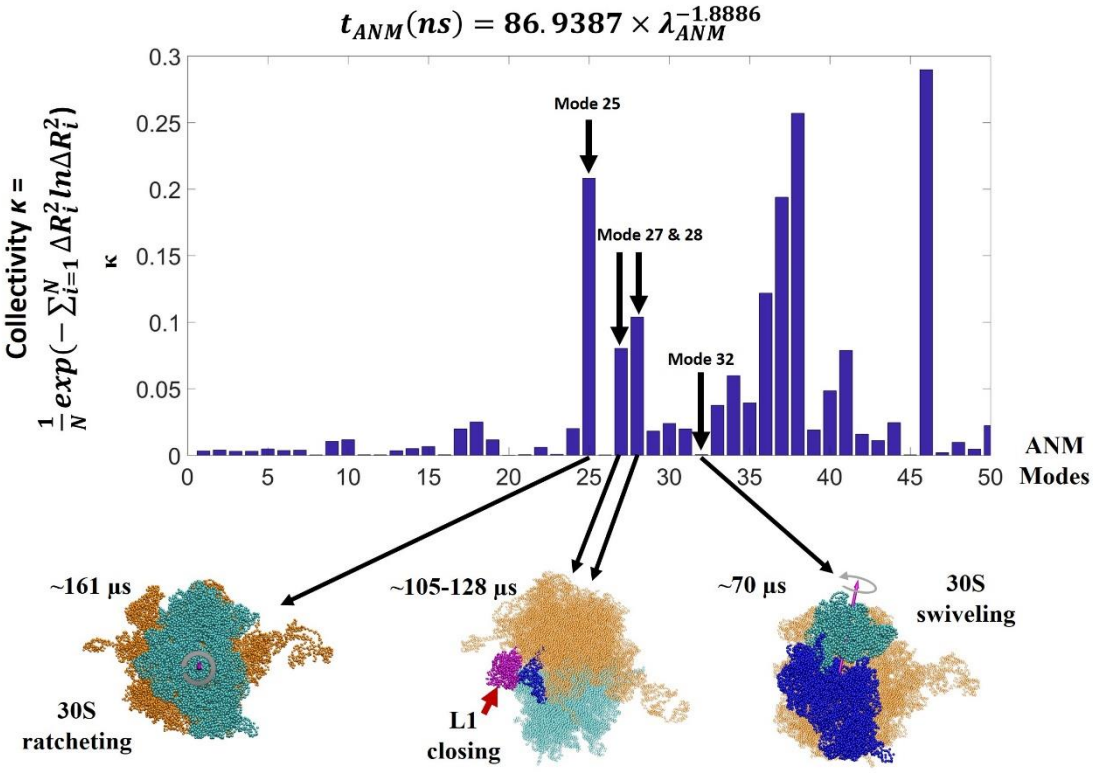


**Figure S5.** The collectivity (**κ**)[13] of the top 50 slowest ANM modes and three discussed functional motions in the ribosome. The 30S ratcheting motion (mode 25) and the L1 stalk closing motion (modes 27 and 28) are found to be highly collective but not the local 30S head swiveling (mode 32).

**Supporting Table**

**Table S1. The top 50 slowest ribosomal motions characterized by ANM**

| | ANM Mode Index | Eigenvalues | Estimated Time Scale (μs) |
|---|---|---|---|
| Slowest motion | 1 | 4.46E-05 | 14293679.65 |
| | 2 | 6.50E-05 | 7033919.39 |
| | 3 | 8.38E-05 | 4352815.56 |
| | 4 | 1.17E-04 | 2320270.70 |
| | 5 | 3.25E-04 | 335825.34 |
| | 6 | 4.08E-04 | 219343.56 |
| | 7 | 5.57E-04 | 121698.60 |
| | 8 | 7.64E-04 | 67024.34 |
| | 9 | 8.93E-04 | 49911.72 |
| | 10 | 1.21E-03 | 28009.81 |
| | 11 | 1.50E-03 | 18632.15 |
| | 12 | 3.69E-03 | 3419.05 |
| | 13 | 3.94E-03 | 3018.11 |
| | 14 | 4.07E-03 | 2840.08 |
| | 15 | 5.35E-03 | 1696.67 |
| | 16 | 6.34E-03 | 1232.63 |
| | 17 | 7.45E-03 | 907.07 |
| | 18 | 8.56E-03 | 698.76 |
| | 19 | 9.20E-03 | 609.14 |
| | 20 | 1.10E-02 | 433.26 |
| | 21 | 1.12E-02 | 420.91 |
| | 22 | 1.22E-02 | 358.64 |
| | 23 | 1.62E-02 | 208.55 |
| | 24 | 1.73E-02 | 185.47 |
| Ratcheting motion | 25 | 1.86E-02 | 160.73 |
| | 26 | 1.91E-02 | 153.34 |
| L1 stalk motion | 27 | 2.10E-02 | 128.19 |
| L1 stalk motion | 28 | 2.33E-02 | 105.09 |
| | 29 | 2.54E-02 | 89.37 |
| | 30 | 2.62E-02 | 84.47 |
| | 31 | 2.76E-02 | 76.61 |
| Head swiveling motion | 32 | 2.90E-02 | 69.91 |
| | 33 | 3.15E-02 | 59.47 |

| | | |
|---|---|---|
| 34 | 3.51E-02 | 48.67 |
| 35 | 3.81E-02 | 41.70 |
| 36 | 4.17E-02 | 35.11 |
| 37 | 4.31E-02 | 33.03 |
| 38 | 5.26E-02 | 22.64 |
| 39 | 5.32E-02 | 22.16 |
| 40 | 5.56E-02 | 20.36 |
| 41 | 5.69E-02 | 19.52 |
| 42 | 6.03E-02 | 17.50 |
| 43 | 6.48E-02 | 15.28 |
| 44 | 6.56E-02 | 14.90 |
| 45 | 6.80E-02 | 13.92 |
| 46 | 6.91E-02 | 13.51 |
| 47 | 7.32E-02 | 12.14 |
| 48 | 7.37E-02 | 11.97 |
| 49 | 7.41E-02 | 11.84 |
| 50 | 7.47E-02 | 11.67 |

ANM is performed on the *Thermus thermophilus* 70S ribosome whose missing atoms, residues and subunits were patched using the individually solved subunits as templates[14]. The estimated time scales of the vibrational modes are obtained from the general time power law for ANM eigenvalues of three proteins (ubiquitin, FGF2 and HPNAP).

**Supporting References**


(1) McQuarrie, D. A. The Time-Correlation Function Formalism II. In *Statistical Mechanics*; University Science Books, 2000; pp 543–592.

(2) Pearson, K. Note on Regression and Inheritance in the Case of Two Parents. *Proc. R. Soc. London* **1895**, *58* (1), 240–242.

(3) Eyal, E.; Chennubhotla, C.; Yang, L.-W.; Bahar, I. Anisotropic Fluctuations of Amino Acids in Protein Structures: Insights from X-Ray Crystallography and Elastic Network Models. *Bioinformatics* **2007**, *23* (13), i175–i184.

(4) Yang, L.-W.; Eyal, E.; Bahar, I.; Kitao, A. Principal Component Analysis of Native Ensembles of Biomolecular Structures (PCA_NEST): Insights into Functional Dynamics. *Bioinformatics* **2009**, *25* (5), 606–614.

(5) Henry, E. R.; Szabo, A. Influence of Vibrational Motion on Solid State Line Shapes and NMR Relaxation. *J. Chem. Phys.* **1985**, *82* (11), 4753.

(6) Best, R. B.; Vendruscolo, M. Determination of Protein Structures Consistent with NMR Order Parameters. *J. Am. Chem. Soc.* **2004**, *126* (26), 8090–8091.

(7) Tjandra, N.; Feller, S. E.; Pastor, R. W.; Bax, A. Rotational Diffusion Anisotropy of Human Ubiquitin from 15N NMR Relaxation. *J. Am. Chem. Soc.* **1995**, *117* (50), 12562–12566.

(8) Yang, L.-W.; Chng, C.-P. Coarse-Grained Models Reveal Functional Dynamics--I. Elastic Network Models--Theories, Comparisons and Perspectives. *Bioinform. Biol. Insights* **2008**, *2*, 25–45.

(9) Yang, L.-W.; Kitao, A.; Huang, B.-C.; Gō, N. Ligand-Induced Protein Responses and Mechanical Signal Propagation Described by Linear Response Theories. *Biophys. J.* **2014**, *107* (6), 1415–1425.

(10) Yang, L.-W. Models with Energy Penalty on Interresidue Rotation Address Insufficiencies of Conventional Elastic Network Models. *Biophys. J.* **2011**, *100* (7), 1784–1793.

(11) Li, H.; Chang, Y.-Y.; Lee, J. Y.; Bahar, I.; Yang, L.-W. DynOmics: Dynomics: Dynamics of Structural Proteome and Beyond. *Nucleic Acids Res.* **2017**.

(12) Yang, L.-W.; Rader, A. J.; Liu, X.; Jursa, C. J.; Chen, S. C.; Karimi, H. A.; Bahar, I. OGNM: Online Computation of Structural Dynamics Using the Gaussian Network Model. *Nucleic Acids Res.* **2006**, *34* (Web Server), W24–W31.

(13) Tama, F.; Sanejouand, Y. H. Conformational Change of Proteins Arising from Normal Mode Calculations. *Protein Eng.* **2001**, *14* (1), 1–6.

(14) Chang, K.-C.; Wen, J.-D.; Yang, L.-W. Functional Importance of Mobile Ribosomal Proteins. *Biomed Res. Int.* **2015**, *2015*, 1–11.